Computational Mechanics (1993) 11, 229–251

Computational Mechanics

Four-noded mixed finite elements, using unsymmetric stresses, for linear analysis of membranes

A. Cazzani* and **S. N. Atluri**
Computational Modeling Center, Georgia Institute of Technology, Atlanta, GA 30332-0356, USA

Abstract. A family of new 4-noded membrane elements with drilling degrees of freedom and unsymmetric assumed stresses is presented; it is derived from a mixed variational principle originally formulated for finite strain analysis and already used in the literature to develop a purely kinematic membrane model. The performance of these elements, investigated through some well established benchmark problems, is found to be fairly good and their accuracy is comparable with that given by models with a larger number of nodal parameters.

1 Introduction

The aim of this paper is to present a few assumed (unsymmetric) stress membrane elements with drilling degrees of freedom, as counterparts of purely kinematic models recently developed by Iura and Atluri (1992).

The introduction of corner drilling rotations to develop improved membrane elements dates back to the mid-60s, but early attempts (see for a list MacNeal and Harder 1988) were disappointingly unsuccessful. In recent years, however, Allman (1984) and Bergan and Felippa (1985) succeeded in establishing good triangular elements with corner rotations.

Since then, a revival of interest on the topic of membrane elements with drilling degrees of freedom (DOFs) resulted and several contributions appeared; for a partial list the interested reader is referred to Ibrahimbegovich, Taylor and Wilson (1990) and to Iura and Atluri (1992).

On the other hand, since the pioneering work of Pian (1964), assumed (symmetric) stress elements, with enhanced performances compared to standard displacement-based elements, are now well established.

Assumed unsymmetric stress models were pioneered by Atluri and Murakawa (1977), Murakawa (1978) and Murakawa and Atluri (1978, 1979); unfortunately their formulation, based on the use of complete polynomial stress functions, as suggested by Fraeijs de Veubeke (1975), leads to elements which are too stiff due to the presence of redundant stress modes; however, considering that when the works were published the concept of stability (the so called LBB condition) was not completely clear and the requirements for building least-order coordinate invariant elements (see Punch 1983, and Rubinstein et al. 1983) had still to be addressed, their approach is still interesting and might originate further investigations.

Recently Cook (1987), Allman (1988), Yunus (1988), Yunus et al. (1989), among others, proposed assumed-symmetric-stress membrane elements with drilling DOFs, based on a modified complementary energy or on a Hellinger–Reissner principle. The rotation field is not present in the original form of the variational principle, but is brought into play by the selection of Allman-type shape functions for the displacements: the displacement field of an 8-noded quadrilateral element is approximated by that of a standard 4-noded element with the addition of 4 corner drilling DOFs.

* On leave from Department of Structural Mechanics and Design Automation, University of Trento, via Mesiano 77, I-38050 Trento

A different approach is instead proposed by Ibrahimbegovich, Taylor and Wilson (1990); a mixed variational principle is used where the variables are the displacement, the *skew-symmetric part* of the stress tensor and the rotation field. The skew-symmetric stresses are chosen to be constant within the element and the rotation is assumed to be independently modeled; however the displacement field is discretized through Allman-type shape functions and, therefore, is not completely independent of the rotation.

In the formulation presented here, the independently assumed fields are the displacements, rotations and generally unsymmetric stresses.

In the next section, the variational principle used to develop the new finite element will be formulated; in Sect. 3 the discretization of the independent variables will be presented. Comparisons with other assumed-stress models are made in Sect. 4 and the results of some meaningful benchmark problems are reported and commented upon in Sect. 5.

2 Formulation of a mixed variational principle

In order to obtain a mixed variational principle for linear elastic analysis involving displacements, rigid rotations and unsymmetric stresses, it seems natural to deduce it from a general non-linear variational principle of the same kind.

However, as it will be shown, when this approach is adopted, the resulting functional is not directly suitable for applications, since it turns out that the complementary energy is no longer a positive definite quadratic form of the stress components. At the element level this prevents the so called **H** matrix (see Punch and Atluri 1984) from being inverted as it is required in assumed-stress mixed formulations, wherein the stress parameters are eliminated at the element level.

To overcome the above problem, a perturbation term needs to be introduced in the functional, to ensure that the complementary energy is still a positive definite quadratic form; in doing so, however, a direct relation between the functionals for non-linear and linear analysis is somehow destroyed.

Another approach is to give up, since the very beginning, the idea of building a variational principle for linear elastic analysis as a limit case of a non-linear one; it is then possible to postulate a set of governing equations (possibly depending on a free parameter) for the linear elastic problem and, going backwards, construct a functional that admits the very same equations as its Euler–Lagrange equations when the stationarity conditions are enforced. It will be shown that the two approaches are equivalent, in the sense that the functional obtained in this way can be reduced, with an appropriate selection of the free parameter/perturbation term, to that obtained through the former approach.

2.1 Derivation of a variational principle for linear elastic analysis from a general non-linear case

Although any general form of a mixed variational principle involving only displacements, rigid rotations and unsymmetric stresses may be reduced, in the framework of a linear elasticity, to one and the same expression, here, consistently with Iura and Atluri (1992), the functional which forms the basis of the current formulation is chosen to be that obtained by Atluri (1979, 1980) for the rate formulations of finite strain problems. It is a Hu-Washizu type functional, whose expression in Cartesian components, when only elastic effects are taken into account, is:

$$\Pi(\dot{u}_i, D_{ij}, W_{ij}, \dot{t}_{ij}) = \int_{V_N} \{\dot{Q}(D_{ij}) - \dot{f}_i \dot{u}_i + \dot{t}_{ji}(\dot{u}_{i,j} - D_{ij} - W_{ij}) - \tfrac{1}{2}\tau^N_{ij} W_{ik} W_{kj} - \tau^N_{ij} W_{ik} D_{kj}\} dV$$
$$- \int_{S_{\sigma N}} \dot{\bar{T}}_i \dot{u}_i dS - \int_{S_{uN}} \dot{T}_i (\dot{u}_i - \dot{\bar{u}}_i) dS \tag{1}$$

where $\dot{u}_i$ is the velocity, D_{ij} the velocity strain tensor, W_{ij} the spin tensor, $\dot{t}_{ij}$ the rate of the nominal (unsymmetric, 1st Piola–Kirchhoff) stress tensor, $\dot{f}_i$ the rate of the body force, τ^N_{ij} the true (Cauchy)

stress tensor at the N-th incremental configuration, $\dot{\bar{T}}_i$ the rate of surface traction on the part, S_{σ_N}, of the contour of the body where tractions are prescribed; and $\dot{T}_i$, $\dot{\bar{u}}_i$ the rate of surface traction and the velocity on the remaining part, S_{u_N}, of the contour of the body where velocities are prescribed; a comma denotes differentiation with respect to the corresponding Cartesian coordinate; and integration is carried out, in the framework of an Updated Lagrangean formulation, with reference to the last (the N-th) known configuration. Moreover the rate potential $\dot{Q}$ is given by

$$\dot{Q}(D_{ij}) = \tfrac{1}{2} D_{ij} L_{ijkl} D_{kl} - \tfrac{1}{2} \tau^N_{ij} D_{ik} D_{kj} \tag{2}$$

where L_{ijkl} is a fourth order tensor of elastic moduli.

For isotropic linearly elastic plane stress problems, or *the first increment* of an otherwise non-linear problem, using the simplified notations: $\dot{u}_i = u_i$, $\dot{t}_{ij} = t_{ij}$, $\tau^N_{ij} = 0$, $D_{ij} = \varepsilon_{ij}$, $W_{12} = -\theta$, $W_{21} = \theta$, etc., the above functional reduces to

$$\begin{aligned} \Pi_1(u_\alpha, \varepsilon_{\alpha\beta}, \theta, t_{\alpha\beta}) = \int_S h \Big\{ & \frac{E}{2(1-\nu^2)}(\varepsilon_{11}^2 + \varepsilon_{22}^2 + 2\nu\varepsilon_{11}\varepsilon_{22}) + \frac{E}{2(1+\nu)}(\varepsilon_{12}^2 + \varepsilon_{21}^2) \\ & + t_{11}(u_{1,1} - \varepsilon_{11}) + t_{22}(u_{2,2} - \varepsilon_{22}) + t_{12}(u_{2,1} - \varepsilon_{21} - \theta) \\ & + t_{21}(u_{1,2} - \varepsilon_{12} + \theta) - f_\alpha u_\alpha \Big\} dS - \int_{C_\sigma} h \bar{T}_\alpha u_\alpha dc - \int_{C_u} h T_\alpha (u_\alpha - \bar{u}_\alpha) dc \end{aligned} \tag{3}$$

where h is the thickness of the membrane (assumed from now on, without loss of generality, equal to unity), E and ν are respectively the Young's modulus and the Poisson's ratio, while greek subscripts, ranging from 1 to 2, are used to denote the coordinates in the plane of the membrane.

It must be noted that in Eq. (3) the strain components are assumed to be *symmetric*, since such are, by definition, the components of the velocity strain D_{ij} in Eq. (1); thus $\varepsilon_{12} = \varepsilon_{21}$, and the symmetry is also inherited by their variations ($\delta\varepsilon_{12} = \delta\varepsilon_{21}$) which are, therefore, not independent. From this functional, Eq. (3), it is possible to derive a Hellinger–Reissner type variational principle by eliminating the strain tensor. One way to do so is to enforce, identically, the condition of stationarity of Π_1 with respect to arbitrary, but *symmetric*, variations of the strain components $\varepsilon_{\alpha\beta}$. The corresponding Euler–Lagrange equations give the constitutive law (CL) for the unsymmetric stress components:

$$\begin{aligned} t_{11} &= \frac{E}{1-\nu^2}(\varepsilon_{11} + \nu\varepsilon_{22}) \\ t_{22} &= \frac{E}{1-\nu^2}(\varepsilon_{22} + \nu\varepsilon_{11}) \\ t_{12} + t_{21} &= \frac{E}{1+\nu}(\varepsilon_{12} + \varepsilon_{21}) = \frac{2E}{1+\nu}\varepsilon_{12}. \end{aligned} \tag{4}$$

As a consequence of the symmetry of $\varepsilon_{\alpha\beta}$, only the symmetric part, $t_{\alpha\beta} + t_{\beta\alpha}$, of the stress tensor enters in the constitutive law and therefore the shear components are not completely determined by the knowledge of the strain components. However, since the strain energy in (3) is still a positive definite quadratic form (for $E > 0$, $|\nu| < 1$), CL can be inverted and expressions for $\varepsilon_{\alpha\beta}$ in terms of $t_{\alpha\beta}$ back-substituted in (3), in order to obtain the following Hellinger–Reissner type functional:

$$\begin{aligned} \Pi_2(u_\alpha, \theta, t_{\alpha\beta}) &= \Pi_1(u_\alpha, \varepsilon_{\alpha\beta}(t_{\gamma\delta}), \theta, t_{\alpha\beta}) \\ &= \int_S \Big\{ -\frac{1}{2E}(t_{11}^2 + t_{22}^2 - 2\nu t_{11} t_{22}) - \frac{1+\nu}{4E}(t_{12} + t_{21})^2 + t_{11}u_{1,1} + t_{22}u_{2,2} \\ &\quad + t_{12}(u_{2,1} - \theta) + t_{21}(u_{1,2} + \theta) - f_\alpha u_\alpha \Big\} dS - \int_{C_\sigma} \bar{T}_\alpha u_\alpha dc - \int_{C_u} T_\alpha (u_\alpha - \bar{u}_\alpha) dc. \end{aligned} \tag{5}$$

It is easy to see that the complementary energy is no longer positive definite: in matrix form one

has indeed:

$$W_c(t_{\alpha\beta}) = \{t_{11} \quad t_{12} \quad t_{21} \quad t_{22}\} \frac{1}{2E} \begin{bmatrix} 1 & & & -\nu \\ & \frac{1+\nu}{2} & \frac{1+\nu}{2} & \\ & \frac{1+\nu}{2} & \frac{1+\nu}{2} & \\ -\nu & & & 1 \end{bmatrix} \begin{Bmatrix} t_{11} \\ t_{12} \\ t_{21} \\ t_{22} \end{Bmatrix} \tag{6}$$

and since the principal minors of the compliance matrix are no longer strictly positive, there will exist some combinations of non vanishing stress components which produce a zero energy state, as pointed out by Fraeijs de Veubeke and Millard (1976). Obviously this holds also when the stress field is discretized and each component is expressed as a linear combination of polynomials depending on some undetermined parameters β_i. As a consequence, since it is not possible to perform a matrix inversion, stress parameters cannot be eliminated at the element level.

To better understand this point, let's consider the Euler–Lagrange equations corresponding to the stationarity of Π_2 w.r.t. arbitrary variations of u_α, $t_{\alpha\beta}$; of course the stress tensor is generally *unsymmetric*, so that the variations of its components are *not* related. With simple manipulations, it turns out that stationarity of Π_2 implies the following:

$$u_{1,1} = \frac{t_{11} - \nu t_{22}}{E}, \quad u_{2,2} = \frac{t_{22} - \nu t_{11}}{E}, \quad u_{2,1} = \frac{1+\nu}{2E}(t_{12} + t_{21}) + \theta \tag{7}$$

$$u_{1,2} = \frac{1+\nu}{2E}(t_{12} + t_{21}) - \theta, \quad t_{12} = t_{21} \tag{8}$$

$$t_{11,1} + t_{21,2} - f_1 = 0, \quad t_{21,1} + t_{22,2} - f_2 = 0 \tag{9}$$

which are respectively the compatibility condition, CC, written in terms of stress components, Eq. (7), the angular momentum balance, AMB, Eq. (8), and the linear momentum balance, LMB, Eq. (9). For sake of completeness, the boundary conditions enforced by the stationarity of (5) are, as usual

$$n_\alpha t_{\alpha\beta} = \bar{T}_\beta \quad \text{on } C_\sigma \tag{10}$$

$$u_\alpha = \bar{u}_\alpha \quad \text{on } C_u \tag{11}$$

i.e. the traction boundary condition (TBC) on that part of the contour where traction are prescribed and the displacement boundary condition (DBC) on that part of the contour where kinematic constraints are prescribed; n_α is a unit outward normal to the contour. The only condition to be satisfied a priori is the constitutive law given by Eqs. (4), used to evaluate strains once stresses are known.

However, as easily seen, the last two of Eqs. (7) cannot be solved for t_{12} and t_{21} separately; it is nonetheless possible to eliminate the stress components from Eq. (5) by means of Eqs. (7) and obtain a functional where only kinematic variables appear:

$$\Pi_3(u_\alpha, \theta) = \Pi_2(u_\alpha, \theta, t_{\alpha\beta}(u_\gamma, \theta)) = \int_S \left\{ \frac{E}{2(1-\nu^2)}(u_{1,1}^2 + u_{2,2}^2 + 2\nu u_{1,1} u_{2,2}) + \frac{E}{1+\nu}(u_{1,2} + \theta)(u_{2,1} - \theta) - f_\alpha u_\alpha \right\} dS + \textit{contour integrals} \tag{12}$$

but in Eq. (12) θ is virtually already eliminated, since, by the last two of Eqs. (7), it results a priori $\theta = (u_{2,1} - u_{1,2})/2$.

The particular structure of Π_2, with the complementary energy depending only on the symmetric part of the stress field, is *not* a result of the particular way to derive it from Eq. (3); indeed

a Hellinger–Reissner variational principle can be deduced directly from Eq. (1) by introducing the following contact transformation:

$$\dot{Q}(D_{ij}) - \dot{t}_{ji} D_{ij} - \tau_{ij}^N W_{ik} D_{kj} = -\dot{R}(\dot{t}_{ij}, W_{ij}) \tag{13}$$

and gives

$$\begin{aligned} \Pi_{HR}(\dot{u}_i, W_{ij}, \dot{t}_{ij}) = & \int_{V_N} \left\{ -\dot{R}(\dot{t}_{ij}, W_{ij}) - \dot{f}_i \dot{u}_i + \dot{t}_{ji}(\dot{u}_{i,j} - W_{ij}) - \frac{1}{2} \tau_{ij}^N W_{ik} W_{kj} \right\} dV \\ & - \int_{S_{\sigma N}} \dot{\bar{T}}_i \dot{u}_i dS - \int_{S_{uN}} \dot{T}_i (\dot{u}_i - \dot{\bar{u}}_i) dS \end{aligned} \tag{14}$$

which, reduced to an isotropic linearly elastic problem, leads again to Eq. (5). Obviously the same happens if Π_2 is derived directly by the corresponding Hellinger–Reissner principle written for the continuum in incremental form, as in Murakawa (1978), or for general shells, as in Atluri (1984); this will be shown in a forthcoming paper.

As a result it seems that *it is not possible* to deduce a mixed variational principle—involving only displacements, rigid rotations, and a priori unsymmetric stresses—for the linear elastic analysis, starting from a general non-linear one.

The rationale can be found in the fact that, when reducing to the linear elastic case, the nominal stress tensor turns out to be a priori *symmetric*: indeed, it can be shown (see Atluri 1980) that

$$\dot{t}_{ij} = \dot{\sigma}_{ij} - (W_{ik} + D_{ik}) \tau_{kj}^N \tag{15}$$

where $\dot{\sigma}_{ij} = j \tau_{ij}^N + \dot{\tau}_{ij}$ is the Kirchhoff stress rate, j the determinant of the rate of the deformation gradient, and $\dot{\tau}_{ij}$ the rate of the true stress. Obviously $\dot{\sigma}_{ij}$ is a priori *symmetric* since such are both τ_{ij}^N and $\dot{\tau}_{ij}$; as a consequence, for a linear elastic analysis—or, which is the same, for the first step of a non-linear one—$\tau_{ij}^N = 0$ and therefore from Eq. (15) it follows $\dot{t}_{ij} = \dot{\tau}_{ij}$, *symmetric*.

To obtain a Hellinger–Reissner principle able to deal with assumed *unsymmetric* stress components, a perturbation term may be inserted inside the functional, in order to ensure that the complementary energy is always positive definite. One way to do so is to introduce some particular initial stress state so that some of the components of τ_{ij}^N are retained when deriving Eq. (5) from Eq. (14); however there are no guidelines to ensure that the resulting complementary energy is free from zero stress energy states; another method is to add to the complementary energy a perturbation term consisting of the square of the skew-symmetric part of the stress tensor multiplied by a strictly positive, but otherwise arbitrary, parameter, γ, in order to obtain:

$$\begin{aligned} \hat{\Pi}_2(u_\alpha, \theta, t_{\alpha\beta}) = & \int_S \left\{ -\frac{1}{2E}(t_{11}^2 + t_{22}^2 - 2\nu t_{11} t_{22}) - \frac{1+\nu}{4E}(t_{12} + t_{21})^2 - \gamma \frac{1+\nu}{4E}(t_{12} - t_{21})^2 \right. \\ & \left. + t_{11} u_{1,1} + t_{22} u_{2,2} + t_{12}(u_{2,1} - \theta) + t_{21}(u_{1,2} + \theta) - f_\alpha u_\alpha \right\} dS \\ & - \int_{C_\sigma} \bar{T}_\alpha u_\alpha dc - \int_{C_u} T_\alpha (u_\alpha - \bar{u}_\alpha) dc. \end{aligned} \tag{16}$$

It is easy to see that the first two CC, Eq. (7), the AMB, Eq. (8) and the LMB, Eq. (9) are still the Euler–Lagrange equations resulting from the stationarity of $\hat{\Pi}_2$, while the last two CC are substituted by:

$$\begin{aligned} u_{2,1} &= \frac{1+\nu}{2E}[(t_{12} + t_{21}) + \gamma(t_{12} - t_{21})] + \theta \\ u_{1,2} &= \frac{1+\nu}{2E}[(t_{12} + t_{21}) - \gamma(t_{12} - t_{21})] - \theta \end{aligned} \tag{17}$$

while the complementary energy, Eq. (6), becomes

$$W_c(t_{\alpha\beta}) = \{t_{11} \quad t_{12} \quad t_{21} \quad t_{22}\} \frac{1}{2E} \begin{bmatrix} 1 & & & -\nu \\ & \frac{1+\nu}{2}(1+\gamma) & \frac{1+\nu}{2}(1-\gamma) & \\ & \frac{1+\nu}{2}(1-\gamma) & \frac{1+\nu}{2}(1+\gamma) & \\ -\nu & & & 1 \end{bmatrix} \begin{Bmatrix} t_{11} \\ t_{12} \\ t_{21} \\ t_{22} \end{Bmatrix} \tag{18}$$

which is positive definite (with the usual restrictions on E and ν) as long as γ is strictly positive. As it is easily seen, for the particular choice $\gamma = 1$, Eqs. (17) become decoupled.

Numerical analyses have shown that the results are almost insensitive to the value of γ, at least for a range of several orders of magnitude ($10^{-3} < \gamma < 10^{4}$).

Clearly the introduction of this perturbation term does not allow, in general, to build consistently a variational principle for non-linear analysis of which Eq. (16) is the linear counterpart, and this is a price to pay; on the other hand, a similar technique has been already successfully applied by Ibrahimbegovich, Taylor and Wilson (1990) for the formulation of a variational principle (originally proposed by Reissner 1965) based on the displacement, rigid rotation, and *skew-symmetric* stress fields.

It is worth noting that the kinematic functional used by Iura and Atluri (1992) can be consistently derived in a more rigorous way by eliminating the stress components from the modified functional $\hat{\Pi}_2$.

2.2 Construction of a variational principle starting from equations governing a linear elastic problem

Although the nominal stress turns out to be a priori symmetric in the limit of linear elasticity, it is nonetheless possible to introduce, for linear elastic analysis, a different stress tensor, $t^*_{\alpha\beta}$, which is still a priori unsymmetric. Thus, a different approach to obtain a mixed functional where displacement u_α, rigid rotation θ and assumed unsymmetric stress $t^*_{\alpha\beta}$ (*no longer* the nominal stress) are the independent variables, is to postulate the existence of a set of governing equations like:

$$\begin{aligned} t^*_{11} &= \frac{E}{1-\nu^2}(u_{1,1} + \nu u_{2,2}), \quad t^*_{22} = \frac{E}{1-\nu^2}(u_{2,2} + \nu u_{1,1}) \\ t^*_{12} &= \frac{E}{(1+\nu)}\left[\frac{1}{2}(u_{1,2} + u_{2,1}) + \alpha(u_{2,1} - u_{1,2} - 2\theta)\right] \\ t^*_{21} &= \frac{E}{(1+\nu)}\left[\frac{1}{2}(u_{1,2} + u_{2,1}) - \alpha(u_{2,1} - u_{1,2} - 2\theta)\right] \end{aligned} \tag{19}$$

(corresponding to the CC expressed in terms of stress components, or even to the CL expressed in terms of displacement gradients and rigid rotation), and the equivalent LMB, Eq. (9), AMB, Eq. (8), TBC, Eq. (10), and DBC, Eq. (11) written in terms of $t^*_{\alpha\beta}$ instead of $t_{\alpha\beta}$. In Eqs. (19) α is an arbitrary, but *strictly positive*, parameter.

It is easy to verify that the following functional:

$$\begin{aligned} \Pi^*_2(u_\alpha, \theta, t^*_{\alpha\beta}) = \int_S \Big\{ & -\frac{1}{2E}(t^{*2}_{11} + t^{*2}_{22} - 2\nu t^*_{11} t^*_{22}) - \frac{1+\nu}{4E}(t^*_{12} + t^*_{21})^2 - \frac{1+\nu}{8\alpha E}(t^*_{12} - t^*_{21})^2 \\ & + t^*_{11} u_{1,1} + t^*_{22} u_{2,2} + t^*_{12}(u_{2,1} - \theta) + t^*_{21}(u_{1,2} + \theta) - f_\alpha u_\alpha \Big\} dS \\ & - \int_{C_\sigma} \bar{T}_\alpha u_\alpha dc - \int_{C_u} T^*_\alpha (u_\alpha - \bar{u}_\alpha) dc \end{aligned} \tag{20}$$

admits the above equations as its Euler–Lagrange and boundary conditions when stationarity is enforced. It is also easy to verify that the functional of Eq. (20) corresponds to $\hat{\Pi}_2$ when the value $\gamma = 1/(2\alpha)$ is chosen for the perturbation parameter; as before, therefore, it is not possible to extend it to cover non-linear problems.

2.3 Variational principle applied to a finite element assembly

So far the continuum problem has been considered; for a finite element discretization it is necessary to take into account the effects of interelement boundaries also. In the following, distributed external forces acting along the interelement contour will not be taken into account and, unless otherwise stated, it will be assumed that the displacement field is at least C^0 continuous across the elements and that the prescribed displacements will be modeled through the same shape functions.

Consequently the DBC will be met a priori, as long as the interelement displacement continuity is met; no restrictions will be imposed, a priori, on the stress field which, generally, is separately modeled over each element, so that traction reciprocity along any interelement boundary is usually violated.

However this traction reciprocity requirement turns out to be included in the functional (5) when it is applied to an assembly of finite elements: indeed the stationarity condition w.r.t. arbitrary variations of the displacement field is, in this case:

$$\delta \Pi_2(u_\alpha, \theta, t_{\alpha\beta}) = 0 = \sum_m \int_{S_m} \{t_{11}\delta u_{1,1} + t_{22}\delta u_{2,2} + t_{21}\delta u_{1,2} + t_{12}\delta u_{2,1} - f_1 \delta u_1 - f_2 \delta u_2\} dS. \tag{21}$$

Now the divergence theorem is applied to each element and introduces the contribution from elements boundaries, ρ_m:

$$\sum_m \int_{S_m} \{t_{11}\delta u_{1,1} + t_{22}\delta u_{2,2} + t_{21}\delta u_{1,2} + t_{12}\delta u_{2,1} - f_1 \delta u_1 - f_2 \delta u_2\} dS$$

$$= \sum_m \int_{S_m} \{-(t_{11,1} + t_{21,2} + f_1)\delta u_1 - (t_{12,1} + t_{22,2} + f_2)\delta u_2\} dS + \sum_m \oint_{\rho_m} \{T_1 \delta u_1 + T_2 \delta u_2\} dc \tag{22}$$

where $T_\alpha = n_\beta t_{\beta\alpha}$ is the traction acting on the boundary of the m-th element, whose outward unit normal is n_β.

Clearly the sum of the boundaries of all the elements gives the external boundary of the body, plus all the interelement boundaries, each counted twice, with unit normals equal and opposite: $n_\beta^+ = -n_\beta^-$. So the terms coming from the contour integration in Eq. (22) add up to give the DBC ($\delta u_1 = \delta u_2 = 0$ on C_u) and the TBC ($T_1 = T_2 = 0$ on C_σ since there are no applied distributed tractions) for the whole body; and as many interelement boundary conditions such as:

$$\int_{\rho_m \cap \rho_n} \{n_\beta (t_{\beta\alpha}^{(m)} - t_{\beta\alpha}^{(n)}) \delta u_\alpha\} dc \tag{23}$$

as the number of interelement boundaries. It is apparent that Eq. (23) constitutes the traction reciprocity condition (TRC), written in its weak form.

It is important to note, as it can be seen from Eq. (22) that LMB, TBC and TRC are all summed up (i.e., each is not *individually* satisfied) in the Euler–Lagrange equation of the variational principle, in the case of an assembly of finite elements; and it is expected that this combined condition of LMB, TBC, and TRC might produce poor results in each of these individual conditions, in the presence of a distorted mesh.

3 The finite element model

In order to implement the variational principle stated in the previous section, it is necessary to develop a finite element model where the three fields, displacement, rigid rotation and *unsymmetric* stress are independently discretized.

3.1 Discretized form of the variational principle

When suitable interpolations are introduced for u_α, θ, $t_{\alpha\beta}$ in terms of undetermined parameters q_i (nodal displacements), ω_i (rotations), β_i (stresses)—written in vector form as $\underline{q}$, $\underline{\omega}$, $\underline{\beta}$ respectively—it follows that the discretized form of Eq. (5) referred to a single element is:

$$\hat{\Pi}_2 = -\tfrac{1}{2}\underline{\beta}^t \cdot \underline{\underline{H}}_{\beta\beta} \cdot \underline{\beta} - \underline{\beta}^t \cdot \underline{\underline{H}}_{\beta\omega} \cdot \omega + \underline{\beta}^t \cdot \underline{\underline{G}} \cdot \underline{q} + \underline{Q}^t \cdot \underline{q} \tag{24}$$

where

$$\tfrac{1}{2}\underline{\beta}^t \cdot \underline{\underline{H}}_{\beta\beta} \cdot \underline{\beta} = \int_S \left\{ \frac{1}{2E}(t_{11}^2 + t_{22}^2 - 2\nu t_{11} t_{22}) + \frac{1+\nu}{4E}(t_{12} + t_{21})^2 + \gamma \frac{1+\nu}{4E}(t_{12} - t_{21})^2 \right\} dS$$

$$\underline{\beta}^t \cdot \underline{\underline{H}}_{\beta\omega} \cdot \underline{\omega} = \int_S \{t_{12}\theta - t_{21}\theta\} dS$$

$$\underline{\beta}^t \cdot \underline{\underline{G}} \cdot \underline{q} = \int_S \{t_{11}u_{1,1} + t_{22}u_{2,2} + t_{12}u_{2,1} + t_{21}u_{1,2}\} dS$$

$$\underline{Q}^t \cdot \underline{q} = -\int_S \{f_\alpha u_\alpha\} dS - \int_{C_\sigma} \bar{T}_\alpha u_\alpha dc$$

where the dot denotes a matrix product and superscript t the transpose of the relevant vector or matrix.

As usual, the stress parameters are eliminated at the element level, while for the rotation parameters both options, to retain them or to eliminate them, should be considered. In the former case, which occurs only when these parameters are nodal variables and the rotation field is continuously modeled across the elements, the following kinematic model is obtained, once stresses are eliminated:

$$\Pi_{q\omega} = \tfrac{1}{2}\underline{q}^t \cdot \underline{\underline{K}}_{qq} \cdot \underline{q} + \underline{q} \cdot \underline{\underline{K}}_{q\omega} \cdot \underline{\omega} + \tfrac{1}{2}\underline{\omega}^t \cdot \underline{\underline{K}}_{\omega\omega} \cdot \underline{\omega} + \underline{Q}^t \cdot \underline{q} \tag{25}$$

with

$$\underline{\underline{K}}_{qq} = \underline{\underline{G}}^t \cdot \underline{\underline{H}}_{\beta\beta}^{-1} \cdot \underline{\underline{G}}; \quad \underline{\underline{K}}_{q\omega} = -\underline{\underline{G}}^t \cdot \underline{\underline{H}}_{\beta\beta}^{-1} \cdot \underline{\underline{H}}_{\beta\omega}; \quad \underline{\underline{K}}_{\omega\omega} = \underline{\underline{H}}_{\beta\omega}^t \cdot \underline{\underline{H}}_{\beta\beta}^{-1} \cdot \underline{\underline{H}}_{\beta\omega}. \tag{26}$$

In the latter case, i.e. when rotation parameters are considered internal ones, not necessarily referred to the nodes, and consequently the rotation field is assumed to be discontinuous across elements, the following displacement model is obtained:

$$\Pi_{qq} = \tfrac{1}{2}\underline{q}^t \cdot \underline{\underline{\tilde{K}}}_{qq} \cdot \underline{q} + \underline{Q}^t \cdot \underline{q} \tag{27}$$

with

$$\underline{\underline{\tilde{K}}}_{qq} = \underline{\underline{G}}^t \cdot \underline{\underline{H}}_{\beta\beta}^{-1} \cdot \underline{\underline{G}} - \underline{\underline{G}}^t \cdot \underline{\underline{H}}_{\beta\beta}^{-1} \cdot \underline{\underline{H}}_{\beta\omega} \cdot (\underline{\underline{H}}_{\beta\omega}^t \cdot \underline{\underline{H}}_{\beta\beta}^{-1} \cdot \underline{\underline{H}}_{\beta\omega})^{-1} \cdot \underline{\underline{H}}_{\beta\omega}^t \cdot \underline{\underline{H}}_{\beta\beta}^{-1} \cdot \underline{\underline{G}} \tag{28}$$

In this way, when the drilling DOFs as internal parameters are eliminated at the element level just like the stress parameters, at the assembly stage the element has exactly the same number and type of DOFs of a standard displacement-based element. So, even if it is required to perform a matrix inversion at the element level in order to build the stiffness matrix, nonetheless the solution procedure is that of a standard stiffness formulation and this proves effective, since it is allowed to mix an element of this type with displacement-formulated ones.

3.2 Choice of discretization of the kinematic fields

Since the main goal of mixed formulations is to improve the accuracy of results—especially in terms of stresses—without the need of increasing the number of nodal variables, it is preferable to model the displacement field as in a standard 4-noded isoparametric element.

The rigid rotation field is, in the present formulation, independent of the displacement field: this means that there are no restrictions on the number of parameters used to discretize it; some reasonable choices—each one giving a different finite element model—are:

—1 parameter model:

$$\theta = [1]\{\omega_1\} \tag{29}$$

the rotation field is therefore constant inside each element and discontinuous across the boundary; physically this DOF can be associated with a rigid rotation of the centroid.
—3 parameters model:

$$\theta = [1 \quad \xi^1 \quad \xi^2] \begin{Bmatrix} \omega_1 \\ \omega_2 \\ \omega_3 \end{Bmatrix}. \tag{30}$$

where ξ^1, ξ^2 are the natural coordinates (referred to the bi-unit square $-1 \leqq \xi^1 \leqq 1, -1 \leqq \xi^2 \leqq 1$ used to define the "parent" element), transformed by the isoparametric mapping into the physical coordinates x^1, x^2 (referred to the "actual" element defined by its corner points $x_i^1, x_i^2, i = 1, \ldots, 4$). The rotation field in Eq. (30) is a complete linear polynomial; however no physical meaning can be associated with the ω_i.
—4 parameters model:

$$\theta = [1 \quad \xi^1 \quad \xi^2 \quad \xi^1\xi^2] \begin{Bmatrix} \omega_1 \\ \omega_2 \\ \omega_3 \\ \omega_4 \end{Bmatrix}. \tag{31}$$

The rotation field (bilinear) is an incomplete quadratic polynomial. In the framework of the isoparametric formulation the same field may be expressed in terms of nodal rotations and, therefore, a physical meaning is associated with these DOFs. However, retaining them as external DOFs, which is equivalent to enforcing the rotation field to be continuous across the elements is neither necessary nor advisable: generally this results in poor performance of the model when more than one elements are assembled together since the relevant AMB conditions are satisfied not individually (in each element), but only in an average sense (over a group of elements), producing a locking effect.
—5 parameters model:

$$\theta = [1 \quad \xi^1 \quad \xi^2 \quad \xi^1\xi^2 \quad (1-(\xi^1)^2)(1-(\xi^2)^2)] \begin{Bmatrix} \omega_1 \\ \omega_2 \\ \omega_3 \\ \omega_4 \\ \omega_5 \end{Bmatrix}. \tag{32}$$

This is an extension of the previous model, Eq. (31) where the introduction of an extra DOF, associated with a bubble-type function (and therefore without a physical meaning) proves effective to relax the continuity requirement of the rotation field across the elements. Thus when an assembly of elements is analyzed, the last DOF is condensed while the others are treated as nodal DOFs: this allows the individual AMB conditions, enforced at the individual element level and not only in an average sense, over a group of elements, to be satisfied in a more accurate way.

3.3 Discretization of the stress field

Once the number d of kinematic parameters (coming from both the displacement and the rotation field) is chosen, a *necessary* requirement for absence of zero energy modes imposes that the number of independent stress modes s has to satisfy:

$$s \geqq d - r \tag{33}$$

where r is the number of rigid body modes. Following the work of Punch (1983), Rubinstein, Punch and Atluri (1983) and Punch and Atluri (1984) it turns out that, provided that stability and invariance

are achieved, the best stress model is a least-order one, i.e. Eq. (33) should be satisfied as an equality, since the introduction of redundant stress modes results generally in a stiffer element. Also, a least order stress selection ($s = d - r$) seems to be optimal both in terms of performances and of use of computer resources.

Least order stress selections are possible for the 1ω, Eq. (29), 3ω, Eq. (30), and 5ω, Eq. (32) models, and will involve 6, 8 or 10 stress modes respectively; for the 4ω model, Eq. (31), however it is not possible to find a suitable 9β stress model, and the same 10 stress modes adopted for the 5ω model will be used instead.

Condition (33) is not sufficient to ensure that zero energy modes will not appear, but their absence can be checked by means of an eigenvalue analysis to verify that the resulting stiffness matrix, Eq. (25) or Eq. (27), has always correct rank.

With reference to a perfect square with sides parallel to centroidal coordinates $\hat{x}^1, \hat{x}^2$ a reasonable selection is:

$$\begin{Bmatrix} t_{11} \\ t_{12} \\ t_{21} \\ t_{22} \end{Bmatrix} = \begin{Bmatrix} \beta_1 + \beta_5 \hat{x}^2 \\ \beta_2 + \beta_7 \hat{x}^2 + \beta_9 \hat{x}^1 \hat{x}^2 \\ \beta_3 + \beta_8 \hat{x}^2 + \beta_{10} \hat{x}^1 \hat{x}^2 \\ \beta_4 + \beta_6 \hat{x}^1 \end{Bmatrix} \tag{34}$$

where the 8β parameters model is obtained when $\beta_9 = \beta_{10} = 0$ and the 6β parameters model when $\beta_7 = \beta_8 = \beta_9 = \beta_{10} = 0$.

The normal stress components are modeled through incomplete linear polynomials, while incomplete second-order polynomials are used for the shear components; in particular the mixed second order terms are necessary to ensure that matrix $\underline{\underline{H}}^t_{\beta\omega} \cdot \underline{\underline{H}}^{-1}_{\beta\beta} \cdot \underline{\underline{H}}_{\beta\omega}$ in Eq. (26) and (28) has always the correct rank.

With this choice of stress modes the element is capable of modeling any state of constant stress and any state of pure bending; moreover the stress modes corresponding to $\beta_1 - \beta_8$ satisfy a priori the LMB in absence of body forces (however this is no more true, in general, if these polynomials are expressed in natural coordinates ξ^1, ξ^2).

The 6β stress selection is a generalization to an unsymmetric stress tensor of Pian's 5β parameters stress model (Pian and Chen 1983; see also Punch 1983 and Punch and Atluri 1984, who obtain the same model with a different procedure).

When the shape of the element is not that of a perfect square, there are several options for defining the stress model and some care is required because some of them lack coordinate invariance while others are not able to model a state of constant stress so that the resulting element cannot pass a patch test.

To understand this issue, let's consider stress components defined in the natural space, (with coordinates ξ^1, ξ^2) where the base vectors are Cartesian, and then transformed into the physical space through the isoparametric mapping. As usual the coordinates of the physical space are again Cartesian.

Even if the isoparametric mapping for 4-noded elements is bilinear

$$x^\Gamma = a_0^\Gamma + a_1^\Gamma \xi^1 + a_2^\Gamma \xi^1 \xi^2 + a_3^\Gamma \xi^2 \tag{35}$$

with

$$\begin{aligned} a_0^\Gamma &= (x_1^\Gamma + x_2^\Gamma + x_3^\Gamma + x_4^\Gamma)/4, \quad a_1^\Gamma = (-x_1^\Gamma + x_2^\Gamma + x_3^\Gamma - x_4^\Gamma)/4 \\ a_2^\Gamma &= (x_1^\Gamma - x_2^\Gamma + x_3^\Gamma - x_4^\Gamma)/4, \quad a_3^\Gamma = (-x_1^\Gamma - x_2^\Gamma + x_3^\Gamma + x_4^\Gamma)/4 \end{aligned} \tag{36}$$

nevertheless stress components in the physical space defined as above turn out to be curvilinear, since their base vectors are a function of position and change orientation from point to point.

Covariant as well as contravariant base vectors can be considered, so that the stress tensor transformed into the physical space can be represented through its contravariant, covariant or mixed convected components; only the first two types are here considered, namely

$$\boldsymbol{\sigma} = \sigma^{\alpha\beta} \boldsymbol{g}_\alpha \boldsymbol{g}_\beta = \sigma_{\alpha\beta} \boldsymbol{g}^\alpha \boldsymbol{g}^\beta \tag{37}$$

the representation in terms of the fixed Cartesian basis is instead:

$$\boldsymbol{\sigma} = t_{\Gamma\Delta}\boldsymbol{e}_\Gamma\boldsymbol{e}_\Delta \tag{38}$$

since $e_\Gamma = \boldsymbol{e}^\Gamma$.

If ξ^1, ξ^2 are convected coordinates, Cartesian in the natural space and x^1, x^2 are the Cartesian coordinates of the physical space, then the relation between covariant convected and Cartesian base vectors is the following:

$$\boldsymbol{g}_\alpha = \frac{\partial x^\Gamma}{\partial \xi^\alpha}\boldsymbol{e}_\Gamma \tag{39}$$

So, in matrix form:

$$\begin{Bmatrix}\boldsymbol{g}_1\\ \boldsymbol{g}_2\end{Bmatrix} = \begin{bmatrix}\dfrac{\partial x^1}{\partial \xi^1} & \dfrac{\partial x^2}{\partial \xi^1}\\ \dfrac{\partial x^1}{\partial \xi^2} & \dfrac{\partial x^2}{\partial \xi^2}\end{bmatrix}\begin{Bmatrix}\boldsymbol{e}_1\\ \boldsymbol{e}_2\end{Bmatrix} = \begin{bmatrix}J_1^1 & J_1^2\\ J_2^1 & J_2^2\end{bmatrix}\begin{Bmatrix}\boldsymbol{e}_1\\ \boldsymbol{e}_2\end{Bmatrix} = [J]\begin{Bmatrix}\boldsymbol{e}_1\\ \boldsymbol{e}_2\end{Bmatrix} \tag{40}$$

where $[J]$ is the Jacobian of the isoparametric transformation (see Cook 1981) and

$$|J| = J_1^1 J_2^2 - J_1^2 J_2^1 = (a_1^1 a_3^2 - a_3^1 a_1^2) + (a_1^1 a_2^2 - a_2^1 a_1^2)\xi^1 + (a_2^1 a_3^2 - a_3^1 a_2^2)\xi^2 \tag{41}$$

its determinant which must be everywhere positive. This allows to invert the Jacobian in order to express the Cartesian base vectors as functions of the convected ones:

$$\begin{Bmatrix}\boldsymbol{e}_1\\ \boldsymbol{e}_2\end{Bmatrix} = \frac{1}{|J|}\begin{bmatrix}J_2^2 & -J_1^2\\ -J_2^1 & J_1^1\end{bmatrix}\begin{Bmatrix}\boldsymbol{g}_1\\ \boldsymbol{g}_2\end{Bmatrix} = [J]^{-1}\begin{Bmatrix}\boldsymbol{g}_1\\ \boldsymbol{g}_2\end{Bmatrix}. \tag{42}$$

On the other hand, if contravariant convected base vectors are used, their relation with the Cartesian ones is:

$$\begin{Bmatrix}\boldsymbol{g}^1\\ \boldsymbol{g}^2\end{Bmatrix} = \frac{1}{|J|}\begin{bmatrix}J_2^2 & -J_2^1\\ -J_1^2 & J_1^1\end{bmatrix}\begin{Bmatrix}\boldsymbol{e}_1\\ \boldsymbol{e}_2\end{Bmatrix} = [J]^{-T}\begin{Bmatrix}\boldsymbol{e}_1\\ \boldsymbol{e}_2\end{Bmatrix} \tag{43}$$

and, inversely

$$\begin{Bmatrix}\boldsymbol{e}_1\\ \boldsymbol{e}_2\end{Bmatrix} = \begin{bmatrix}J_1^1 & J_2^1\\ J_1^2 & J_2^2\end{bmatrix}\begin{Bmatrix}\boldsymbol{g}^1\\ \boldsymbol{g}^2\end{Bmatrix} = [J]^T\begin{Bmatrix}\boldsymbol{g}^1\\ \boldsymbol{g}^2\end{Bmatrix}. \tag{44}$$

Now, by making use of Eqs. (40)–(44), it is possible to transform any stress state from Cartesian to convected bases and vice-versa; for instance a uniaxial constant stress state whose expression in Cartesian components is (see Punch 1983)

$$\boldsymbol{\sigma} = t_{\Gamma\Delta}\boldsymbol{e}_\Gamma\boldsymbol{e}_\Delta = k\boldsymbol{e}_1\boldsymbol{e}_1 = \begin{bmatrix}k & 0\\ 0 & 0\end{bmatrix}\boldsymbol{e}_\Gamma\boldsymbol{e}_\Delta \tag{45}$$

becomes in contravariant convected components

$$\boldsymbol{\sigma} = \sigma^{\alpha\beta}\boldsymbol{g}_\alpha\boldsymbol{g}_\beta = \frac{k}{|J|^2}\begin{bmatrix}(J_2^2)^2 & -J_1^2 J_2^2\\ -J_1^2 J_2^2 & (J_1^2)^2\end{bmatrix}\boldsymbol{g}_\alpha\boldsymbol{g}_\beta \tag{46}$$

while the covariant convected components are:

$$\boldsymbol{\sigma} = \sigma_{\alpha\beta}\boldsymbol{g}^\alpha\boldsymbol{g}^\beta = k\begin{bmatrix}(J_1^1)^2 & J_1^1 J_2^1\\ J_1^1 J_2^1 & (J_2^1)^2\end{bmatrix}\boldsymbol{g}^\alpha\boldsymbol{g}^\beta. \tag{47}$$

As a result, in the contravariant component representation, Eq. (46), a constant Cartesian stress state is no more expressed, generally, by means of simple polynomials but by rational functions, due to the presence of $|J|^2$, a quadratic polynomial as shown by Eq. (41), in the denominator; the

covariant component representation, Eq. (47), is still expressed by means of polynomials even if the presence of quadratic terms would generally require the use of a higher number of stress parameters.

These considerations are useful for the construction of the stress model when the shape of the element is irregular; a 10 parameters stress model is sought which reduces to Eq. (34) in the limit as the distortion of the element angles goes to zero. The model has to be coordinate-invariant and be able to reproduce any state of constant Cartesian stress: under these conditions the element can behave isotropically and pass the patch test.

If stresses are modeled directly in Cartesian coordinates, referred to the centroid of the elements with the same shape functions of Eq. (34), the resulting stiffness matrix of the element is not coordinate invariant (Punch 1983), since the stress field is not modeled through complete polynomials; moreover the stress distribution is insensitive to distortion of the element shape: the patch test is passed but for non-uniform stress states a locking effect which increases with the severity of mesh distortion should be expected (see Fig. 1).

Coordinate invariance of the stiffness matrix is achieved if the components of the stress model are expressed in the natural coordinates: indeed, being formulated in the natural space, the stress distribution is insensitive to any translation and/or rotation of the physical coordinates and, moreover, the particular choice of the stress modes ensures that the stress components have the *same* expression regardless on the orientation of the ξ^1, ξ^2 axes (i.e. regardless on the way that the "parent" element is mapped into the actual one). There are, however, several ways to express the stress components in natural coordinates, namely:

—Stress shape functions are expressed in the natural coordinates, but stress components are assumed to be Cartesian:

$$\boldsymbol{\sigma} = \begin{bmatrix} \beta_1 + \beta_5\xi^2 & \beta_2 + \beta_7\xi^2 + \beta_9\xi^1\xi^2 \\ \beta_3 + \beta_8\xi^1 + \beta_{10}\xi^1\xi^2 & \beta_4 + \beta_6\xi^1 \end{bmatrix} \boldsymbol{e}_\Gamma \boldsymbol{e}_\Delta. \tag{48}$$

—Stress shape functions are expressed in the natural coordinates, and are assumed to be contravariant (curvilinear) convected components:

$$\boldsymbol{\sigma} = \begin{bmatrix} \sigma^{11} & \sigma^{12} \\ \sigma^{21} & \sigma^{22} \end{bmatrix} \boldsymbol{g}_\gamma \boldsymbol{g}_\delta = \begin{bmatrix} \beta_1 + \beta_5\xi^2 & \beta_2 + \beta_7\xi^2 + \beta_9\xi^1\xi^2 \\ \beta_3 + \beta_8\xi^1 + \beta_{10}\xi^1\xi^2 & \beta_4 + \beta_6\xi^1 \end{bmatrix} \boldsymbol{g}_\gamma \boldsymbol{g}_\delta. \tag{49}$$

so that the Cartesian components are, by Eq. (40):

$$\begin{aligned} t_{11} &= (J_1^1)^2\sigma^{11} + J_1^1 J_2^1(\sigma^{12} + \sigma^{21}) + (J_2^1)^2\sigma^{22} \\ t_{12} &= J_1^1 J_1^2\sigma^{11} + J_1^1 J_2^2\sigma^{12} + J_1^2 J_2^1\sigma^{21} + J_2^1 J_2^2\sigma^{22} \\ t_{21} &= J_1^1 J_1^2\sigma^{11} + J_1^2 J_2^1\sigma^{12} + J_1^1 J_2^2\sigma^{21} + J_2^1 J_2^2\sigma^{22} \\ t_{22} &= (J_1^2)^2\sigma^{11} + J_1^2 J_2^2(\sigma^{12} + \sigma^{21}) + (J_2^2)^2\sigma^{22}. \end{aligned} \tag{50}$$

—Stress shape functions are expressed in the natural coordinates, and are assumed to be covariant (curvilinear) convected components:

$$\boldsymbol{\sigma} = \begin{bmatrix} \sigma_{11} & \sigma_{12} \\ \sigma_{21} & \sigma_{22} \end{bmatrix} \boldsymbol{g}^\gamma \boldsymbol{g}^\delta = \begin{bmatrix} \beta_1 + \beta_5\xi^2 & \beta_2 + \beta_7\xi^2 + \beta_9\xi^1\xi^2 \\ \beta_3 + \beta_8\xi^1 + \beta_{10}\xi^1\xi^2 & \beta_4 + \beta_6\xi^1 \end{bmatrix} \boldsymbol{g}^\gamma \boldsymbol{g}^\delta \tag{51}$$

so that the Cartesian components are, by Eq. (43):

$$t_{11} = \frac{1}{|J|^2}[(J_2^2)^2\sigma_{11} - J_1^2 J_2^2(\sigma_{12} + \sigma_{21}) + (J_1^2)^2\sigma_{22}]$$

$$t_{12} = \frac{1}{|J|^2}[-J_2^1 J_2^2\sigma_{11} + J_1^1 J_2^2\sigma_{12} + J_1^2 J_2^1\sigma_{21} - J_1^1 J_1^2\sigma_{22}]$$

$$t_{21} = \frac{1}{|J|^2}[-J_2^1 J_2^2 \sigma_{11} + J_1^2 J_2^1 \sigma_{12} + J_1^1 J_2^2 \sigma_{21} - J_1^1 J_1^2 \sigma_{22}]$$

$$t_{22} = \frac{1}{|J|^2}[(J_2^1)^2 \sigma_{11} - J_1^1 J_2^1 (\sigma_{12} + \sigma_{21}) + (J_1^1)^2 \sigma_{22}] \tag{52}$$

—Stress shape functions are expressed in the natural coordinates, and are assumed to be contravariant components referred to the centroidal base vectors:

$$\boldsymbol{\sigma} = \begin{bmatrix} \sigma^{11} & \sigma^{12} \\ \sigma^{21} & \sigma^{22} \end{bmatrix} \hat{\boldsymbol{g}}_\gamma \hat{\boldsymbol{g}}_\delta = \begin{bmatrix} \beta_1 + \beta_5 \xi^2 & \beta_2 + \beta_7 \xi^2 + \beta_9 \xi^1 \xi^2 \\ \beta_3 + \beta_8 \xi^1 + \beta_{10} \xi^1 \xi^2 & \beta_4 + \beta_6 \xi^1 \end{bmatrix} \hat{\boldsymbol{g}}_\gamma \hat{\boldsymbol{g}}_\delta \tag{53}$$

and the Cartesian components are still given by Eq. (50) but with the Jacobian components evaluated at the centroid and therefore constant.

—Stress shape functions are expressed in the natural coordinates, and are assumed to be covariant components referred to the centroidal base vectors:

$$\boldsymbol{\sigma} = \begin{bmatrix} \sigma_{11} & \sigma_{12} \\ \sigma_{21} & \sigma_{22} \end{bmatrix} \hat{\boldsymbol{g}}^\gamma \hat{\boldsymbol{g}}^\delta = \begin{bmatrix} \beta_1 + \beta_5 \xi^2 & \beta_2 + \beta_7 \xi^2 + \beta_9 \xi^1 \xi^2 \\ \beta_3 + \beta_8 \xi^1 + \beta_{10} \xi^1 \xi^2 & \beta_4 + \beta_6 \xi^1 \end{bmatrix} \hat{\boldsymbol{g}}^\gamma \hat{\boldsymbol{g}}^\delta \tag{54}$$

where, similarly, the Cartesian components are given by Eq. (52) when the components of the Jacobian are evaluated at the centroid.

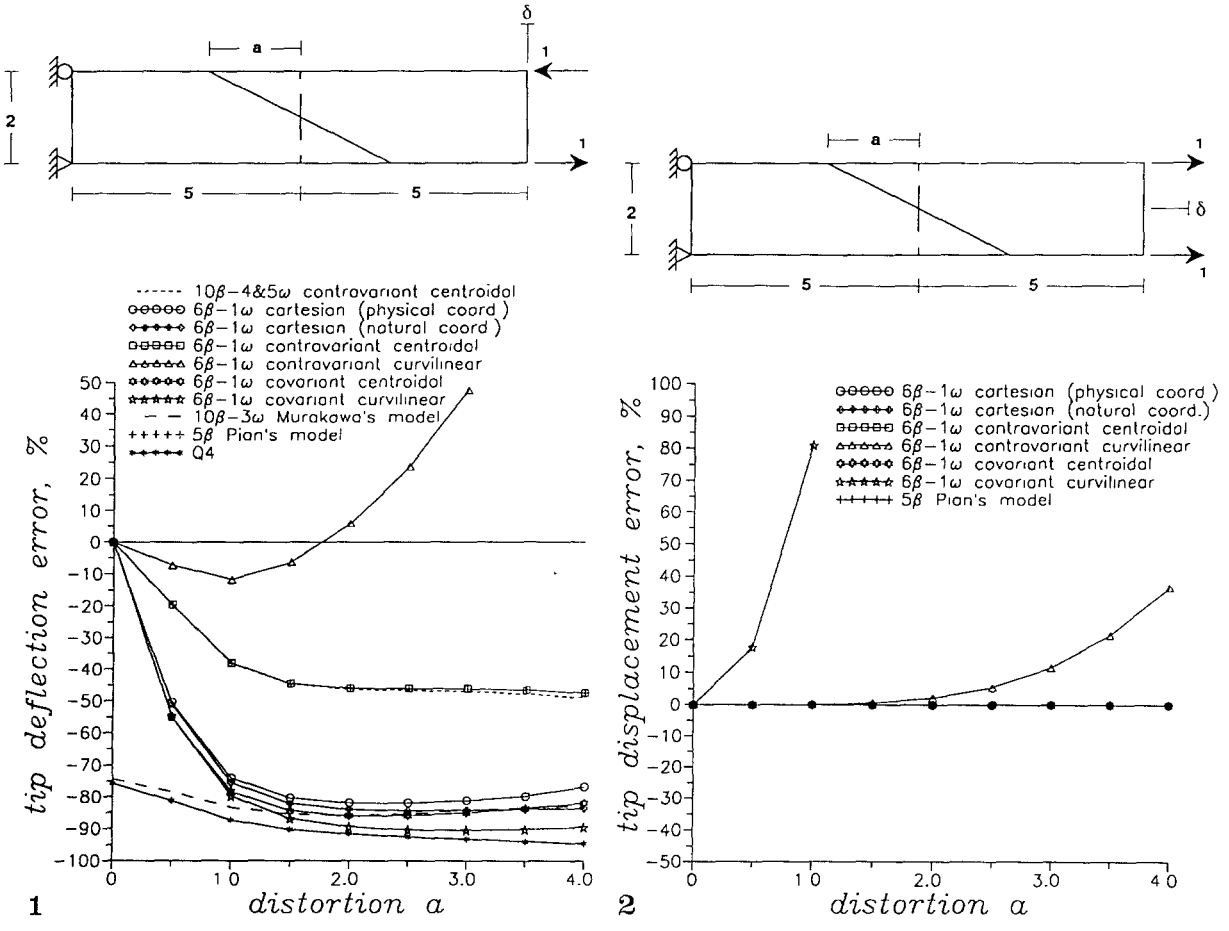

Figs. 1 and 2. Distortion sensitivity analysis **1** in a pure bending problem for several stress models; **2** in a uniform extension problem for several stress models. Material properties are: $E = 1.0$, $\nu = 0.0$

The selection of Eq. (48) gives an element which is both coordinate invariant and passes the patch test, but due to the limited sensitivity to distortion, locking effects should be expected to take place when non-uniform stress are analyzed with an irregular mesh.

On the other hand, selection of a stress model where shape functions are used to define contravariant curvilinear components, Eq. (49), leads to an element which is coordinate invariant but cannot pass the patch test, since, as noted when looking at Eq. (46), the images in the ξ^1, ξ^2 space of polynomials of order zero and one in the x^1, x^2 space are, in general, rational functions and no more polynomials. A similar comment does apply to the choice of Eq. (51), since, as Eq. (47) shows, it would be necessary to have at least complete quadratic polynomials in the natural space to model a constant Cartesian stress state; moreover, the integration involved in the functional (16) which is to be performed numerically cannot give the exact result, if standard Gaussian rules are used due to the presence of a generally non-constant denominator in Eq. (52).

This is the reason that justifies the adoption of a stress model defined in terms of contravariant or covariant components which are referred to a fixed, centroidal, and generally skew system of base vectors and not, as before, to a general curvilinear one. Since the Jacobian components are now constant, it turns out, looking at Eqs. (46), (47), (50) and (52), that each of these approximation allows to formulate a finite element which passes both the coordinate invariance and the patch test. However (see Pian 1985) the stress model cannot satisfy in general the equilibrium equation pointwise, except at the centroid (where it is always satisfied) or when special conditions are fulfilled, like presence of constant stress modes only, or particular restrictions on the shape distortion of the element. It should be noted that the two stress models (53), (54) are different and cannot be reduced, in general, to the same one.

The results produced by these possible choices of stress models are reported in Figs. 1 and 2 where a comparison is made with reference to sensitivity to mesh distortion for the two cases of pure bending and uniform extension respectively.

It appears that the best choice among those previously outlined is the use of a contravariant centroidal stress components model and this will be adopted for all subsequent computations.

4 Comparison with other assumed-stress finite element models

Among the family of new elements proposed here, the $6\beta - 1\omega$ one is similar to that proposed by Pian and Sumihara (1984), Pian (1985), Pian and Tong (1986) and Pian and Wu (1988)—and, independently, by Rubinstein et al. (1983), and Punch and Atluri (1984)—where a *symmetric* stress model depending on 5β parameters, based on a Hellinger–Reissner functional without drilling DOFs, is proposed. Interestingly, the approach introduced by Pian and his coworkers starts from the definition of a complete symmetric (9β parameters) linear stress model in the natural coordinates, whose components are assumed to be Cartesian, and then through the use of incompatible displacement functions they enforce equilibrium condition in order to decouple LMB and TRC from the Euler–Lagrange equations of their Hellinger–Reissner principle. This results in 4 constraint conditions between the stress parameters, which allow to reduce the independent stress modes to only 5: as noted by Pian and Sumihara (1984), however, this approach is equivalent to directly introducing the stress model in the contravariant centroidal components and then transform these into physical, Cartesian components. Under this point of view the choice of contravariant centroidal components is optimal in the sense that they are able to better approximate equilibrium (in a weak sense) with a minimum number of free parameters.

The stress model adopted for the $6\beta - 1\omega$ element is however different in that the stress components are not assumed, a priori, to be symmetric and also the constant part of the stress field is transformed according to Eq. (52) with the Jacobian evaluated at the centroid, so that the stress parameters are generally coupled; anyway the particular discretization of the rotation field, Eq. (29) ensures that the AMB condition has to be satisfied also in its strong form within each element, i.e. the stress tensor in the solution becomes symmetric.

Assumed-unsymmetric-stress elements as introduced by Atluri and Murakawa (1977), Murakawa (1978), and Murakawa and Atluri (1978, 1979) have been used in the framework of incremental

large deformation analysis of compressible and incompressible elastic solids. The formulation is based on a modified complementary energy principle where displacement, rigid rotation and unsymmetric stress are the independent variables. For the displacement field, a standard 4-noded isoparametric model is selected. The rotation field is discretized through internal parameters, without a specific physical meaning, defined as the coefficients of a complete polynomial expansion of the rotation field; completeness here and in the stress representation is sought in order to ensure coordinate invariance of the element. The *unsymmetric* stress components must satisfy a priori the LMB and are derived from first order, i.e. once differentiable, Cartesian stress functions, expressed as complete polynomials in the physical coordinates $\hat{x}^1, \hat{x}^2$:

$$t_{11} = \psi_1(\hat{x}^1, \hat{x}^2)_{,2}, \quad t_{12} = \psi_2(\hat{x}^1, \hat{x}^2)_{,2}, \quad t_{21} = -\psi_1(\hat{x}^1, \hat{x}^2)_{,1}, \quad t_{22} = -\psi_2(\hat{x}^1, \hat{x}^2)_{,1}. \tag{55}$$

Depending on the choice of their order, the number of stress parameters is automatically determined: so for a linear, quadratic, cubic selection of stress functions, the corresponding number of stress parameters will be 4, 10 or 18 (obviously the stress functions are defined to within a constant, since the zero-order term does not give any contribution); except for the 4 stress-parameters model, which is always rank-deficient, all the other elements have redundant stress modes and consequently their response is generally too stiff. For comparison purposes the $10\beta - 3\omega$ model has been implemented: the rotation field is defined as:

$$\theta = [1 \quad \hat{x}^1 \quad \hat{x}^2] \begin{Bmatrix} \omega_1 \\ \omega_2 \\ \omega_3 \end{Bmatrix} \tag{56}$$

i.e. similar to Eq. (30) but with natural coordinates substituted by the physical ones. The stress functions are expressed as:

$$\psi_1 = \beta_1 \hat{x}^1 + \beta_3 \hat{x}^2 + \beta_5 (\hat{x}^1)^2 + \beta_7 \hat{x}^1 \hat{x}^2 + \beta_9 (\hat{x}^2)^2$$
$$\psi_2 = \beta_2 \hat{x}^1 + \beta_4 \hat{x}^2 + \beta_6 (\hat{x}^1)^2 + \beta_8 \hat{x}^1 \hat{x}^2 + \beta_{10} (\hat{x}^2)^2$$

the corresponding stress components, by virtue of Eq. (55), are:

$$t_{11} = \beta_3 + \beta_7 \hat{x}^1 + 2\beta_9 \hat{x}^2, \qquad t_{12} = \beta_4 + \beta_8 \hat{x}^1 + 2\beta_{10} \hat{x}^2$$
$$t_{21} = -\beta_1 - 2\beta_5 \hat{x}^1 - \beta_7 \hat{x}^2, \quad t_{22} = -\beta_2 - 2\beta_6 \hat{x}^1 - \beta_8 \hat{x}^2 \tag{57}$$

and already satisfy LMB. This requirement results in an element which is somehow overconstrained regardless of its shape, as it is shown by the eigenvalue analysis (see Table 3), and is also apparent from the results depicted in Fig. 1: in absence of distortion the element is nonetheless unable to correctly model a state of pure bending; on the other hand, no substantial improvement of the performance can be achieved if Eqs. (57) are rewritten in natural coordinates and the corresponding stress tensor is assumed to be expressed in contravariant centroidal components.

A different approach for the formulation of a stress-based element with drilling DOFs is introduced by Cook (1987), Yunus (1988), Yunus et al. (1989). In the first paper an assumed-symmetric-stress triangular element is developed from the complementary energy principle; the stress model is equilibrated within the element (in absence of body forces) and displacements are then introduced to enforce the equilibrium along the boundary in terms of boundary tractions. The stresses are defined in terms of local, centroidal (not convected) coordinates and each element results from the assembly of three triangular subelements, in order to achieve coordinate invariance. The displacements are modeled by means of Allman-type shape functions, i.e. they are assumed to depend on corner nodal displacements and on some corner nodal drilling DOFs deduced by condensing the mid-side nodal displacements of a 6-noded triangular element (see Allman 1984). Since the nodal drilling DOFs are not true rotations, in the sense that they are not independent of the displacement parameters, it turns out that the element has always a spurious zero-energy mode corresponding to a mechanism in which all the drilling parameters are the same; as a consequence in a finite element mesh it is necessary to restrain at least one of these parameters by fixing its value.

In the two following papers (Yunus 1988 and Yunus et al. 1989), the assumed-symmetric-stress triangular element and a quadrilateral one are deduced from a Hellinger–Reissner variational principle, i.e. following a mixed approach. As in the previous case, drilling DOFs are introduced in the formulation by the choice of Allman-type shape functions for the displacements, not by the particular structure of the functional, as it happens in (5) where rotational parameters are necessary to enforce AMB; this explains how drilling DOFs can coexist with an a priori symmetric stress model. The complete linear assumed-stress model (depending on 9 unconstrained β parameters) is chosen to be expressed in contravariant convected components, as in Eq. (50), but in order to pass the patch test a reduced integration (2×2 Gaussian quadrature rule) must be used; here the reduced integration plays the same role as the use of centroidal components outlined in the previous section (with reference to the formulation of the new element), allowing the element to model a constant Cartesian stress state. However a spurious zero energy mode is still present and that's why at least one drilling DOF has to be fixed in the mesh.

This reason, and the difficulties connected with imposing boundary conditions in terms of rotations (the drilling DOFs associated with the Allman shape functions are not true rotations: see Allman 1988) suggest one not to use this type of shape functions, though effective in dealing with in-plane bending problems, in the development of the finite elements presented in the previous section.

5 Examples

In this section the results of some simple benchmark problems will be presented, in order to assess the reliability of the proposed finite element formulation. Most of the test cases are taken from Pian and Sumihara (1984), MacNeal and Harder (1985) and Ibrahimbegovich et al. (1990).

All numerical integrations are performed by means of a 3×3 Gaussian quadrature rule which, for the particular choice of shape functions employed, turns out to give the same results obtained by analytical integration; moreover the perturbation term γ in Eq. (16) has been taken equal to 1.

To obtain a meaningful comparison of the performance of the present elements with respect to the others, for any given problem the results will be expressed in terms of the total number of external DOFs used in the mesh, before imposing the boundary conditions. This method, used also by Cook (1986), allows one to draw conclusions checking the performance against the total cost of the analysis (i.e. the use of computer resources), and makes possible to compare elements with a different number of DOFs, like in the present case (see Table 1). However, since only the *total* number of external DOFs is evaluated, small discrepancies in the way of imposing the constraints due to a specific type of element do not affect the comparison.

Table 1. Basic properties of the elements used for the numerical tests

Element	Number of nodal DOFs	Number of stress parameters	Number of rotation parameters
Allman (AQ)	12	0	4
Ibrahimbegovich et al. (M)	12	1	4
Iura and Atluri (M1)	12	0	4
Iura and Atluri (M2)	12	0	4
MacNeal and Harder	12	0	4
Pian and Sumihara	8	5	0
Q4	8	0	0
Yunus (Mixed AQ)	12	9	4
Present ($6\beta - 1\omega$)	8	6	1
Present ($8\beta - 3\omega$)	8	8	3
Present ($10\beta - 4\omega$)	8	10	4
Present ($10\beta - 5\omega$)	12	10	5

5.1 *Eigenvalue analysis*

The eigenvalues of the stiffness matrix of a single perfect square element for $E = 1$ and different values of ν in the range 0 to 0.5 have been evaluated analytically by means of a program able to perform algebraic computations in symbolic form and are reported in Table 2: the results clearly show that the stiffness matrix has always correct rank; the results are the same for all the models with 8 external DOFs ($6\beta - 1\omega$, $8\beta - 3\omega$ and $10\beta - 4\omega$), where the rotation parameters are condensed at the element level. The $10\beta - 5\omega$ model (with 12 external DOFs) should be used only when more elements are assembled together, since the AMB condition relative to the fifth parameter is not independent of the others when only a single element is considered.

In Table 3 the non-zero eigenvalues of the present elements with 8 DOFs and of the model proposed by Pian and Sumihara (1984) are numerically evaluated in the case of a perfect square with $E = 1$ and $\nu = 0.3$ and it is found that they coincide; for comparison purposes also the eigenvalues, obtained by Murakawa (1978) for the same geometric and material properties and for elements with several combinations of stress and rotation parameters, are reported; in general the eigenvalues corresponding to flexural modes are too high and this results in a too stiff response when bending is the dominant state.

5.2 *Patch tests*

The elements can pass the single element patch test with a *minimum* number of constraints: a single trapezoidal (skewed) element with one side constrained (2 displacement components fixed at first node and 1 at the other, as in Ibrahimbegovich, Taylor and Wilson 1990) and subject to uniform

Table 2. Eigenvalues (analytically evaluated) for a perfect square element as a function of the Poisson's ratio ($6\beta - 1\omega$, $8\beta - 3\omega$, $10\beta - 4\omega$ models)

Mode	$\nu = 0.0$	$\nu = 0.1$	$\nu = 0.2$	$\nu = 0.3$	$\nu = 0.4$	$\nu = 0.5$
Rigid trans. I	0	0	0	0	0	0
Rigid trans. II	0	0	0	0	0	0
Rigid rotation	0	0	0	0	0	0
Bending I	1/3	1/3	1/3	1/3	1/3	1/3
Bending II	1/3	1/3	1/3	1/3	1/3	1/3
Shear I	1	10/11	5/6	10/13	5/7	2/3
Shear II	1	10/11	5/6	10/13	5/7	2/3
Uniform ext.	1	10/9	5/4	10/7	5/3	2

Table 3. Eigenvalues of a perfect square element (with $E = 1$, $\nu = 0.3$) for several models; β, ω, DOFs refer respectively to the number of stress, rotation and nodal degrees of freedom parameters

Element	Pian and Sumihara	Present	Murakawa (I)	Murakawa (II) and (IV)	Murakawa (III) and (V)
β, ω, DOFs	(5,0,8)	(6,1,8) (8,3,8) (10,4,8)	(4,1,8)	(10,1,8) and (18,1,8)	(10,3,8) and (18,3,8)
Bending I	0.333	0.333	0.000	1.367	0.373
Bending II	0.333	0.333	0.000	1.367	0.373
Shear I	0.769	0.769	0.769	0.769	0.769
Shear II	0.769	0.769	0.769	0.769	0.769
Uniform ext.	1.429	1.429	1.282	1.282	1.282
Trace	3.634	3.634	2.872	5.606	3.566

tension applied to the opposite side gives the exact response in terms of both displacements and stresses for the 8 DOFs models.

For an assembly of elements, two different patch tests can be devised: in the former a square plate consisting of four distorted elementsis subjected to uniform tension (see Iura and Atluri 1992); in the latter a rectangular plate is divided into five elements, one of which is completely surrounded by the other ones and has no nodes on the contour of the plate, is subjected to prescribed boundary displacements (see MacNeal and Harder 1985). For both these problems the element gives the exact solution.

5.3 *A simply supported beam*

With this test the ability of the proposed models to deal with uniaxial bending is checked in the presence of regular and distorted meshes; the material data are: $E = 100$ and $v = 0$, while geometry and loads are sketched in Fig. 3. As shown in Table 4, for the case of regular mesh the value of the midspan deflection is exact; when the mesh is distorted, the relative error is less than 7% for the 8 DOFs models (and this result is more accurate than those obtained with any other model) and about 34% for the 12 DOFs model.

5.4 *A thin cantilever beam*

This very thin cantilever with a moment applied to the free end (see Fig. 4) is another pure bending test, but unlike the previous one, the effect of the Poisson's ratio is here taken into account ($E = 3.0 \times 10^7$, $v = 0.30$). The results reported in Table 5 show that, when the mesh is distorted, this is the most critical test for the elements (if the mesh is undistorted, the theoretically exact solution is always obtained). On the other hand, if a comparison is made with other similar models available in the literature, it appears that only those based on Allman-type shape functions (see Allman 1988), whose drawbacks are outlined in Iura and Atluri (1992), give relatively acceptable

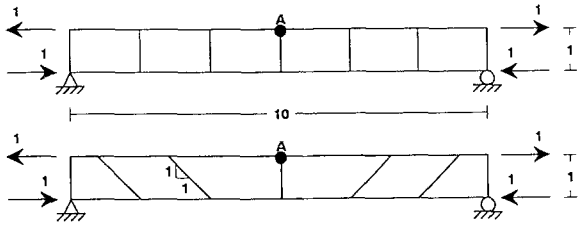

Fig. 3. Regular and distorted mesh for the analysis of the simply supported beam problem. Midspan deflection is referred to point *A*

Table 4. Midspan deflection at *A* for the simply supported beam problem

Element	No. of DOFs	Regular Mesh	Distorted Mesh
Exact	—	1.5	1.5
Ibrahimbegovich et al.	42	1.5	1.14045
Iura and Atluri (M1)	42	1.5	1.0910
Iura and Atluri (M2)	42	1.5	1.0495
Q4	28	0.6279	0.2523
Present ($6\beta - 1\omega$)	28	1.5	1.3994
Present ($8\beta - 3\omega$)	28	1.5	1.3994
Present ($10\beta - 4\omega$)	28	1.5	1.3994
Present ($10\beta - 5\omega$)	42	1.5	0.9809

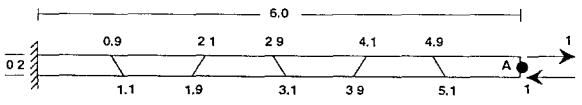

Fig. 4. Distorted mesh used for the analysis of the thin cantilever beam problem

Table 5. Tip deflection at A for the thin cantilever beam problem (distorted mesh), normalized on the exact value

Element	No. of DOFs	v_A
Iura and Atluri (M1)	42	0.10
Iura and Atluri (M2)	42	0.07
Pian and Sumihara	28	0.16
Q4	28	0.02
Yunus (Mixed Aq)	42	0.85
Yunus et al. (AQ)	42	0.82
Present ($6\beta - 1\omega$)	28	0.16
Present ($8\beta - 3\omega$)	28	0.16
Present ($10\beta - 4\omega$)	28	0.16
Present ($10\beta - 5\omega$)	42	0.16

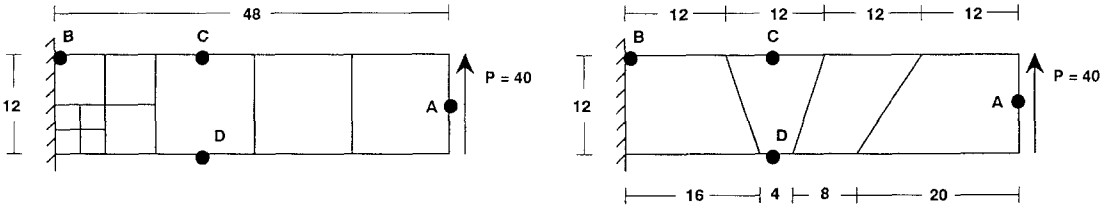

Fig. 5. Regular and distorted mesh for the analysis of the shear-loaded thick cantilever beam problem. Point A is used to evaluate the tip deflection, point B, C and D for stress computations. The pattern of mesh refinement is partially shown in the regular mesh

Table 6. Axial normal stresses at locations B, C, D for the shear-loaded beam test problem

Element	Mesh	No. of DOFs	σ_B	σ_C	σ_D
Exact	—	—	−80.00	−50.00	+50.00
Yunus (Mixed AQ)	4 × 1	30	−71.90	−50.00	+50.00
Yunus et al. (AQ)	4 × 1	30	−70.00	−50.00	+50.00
Present ($8\beta - 3\omega$)	4 × 1	20	−70.00	−50.00	+50.00
Present ($8\beta - 3\omega$)	8 × 2	54	−74.54	−49.98	+49.98
Present ($8\beta - 3\omega$)	16 × 4	170	−80.58	−50.00	+50.00
Present ($10\beta - 5\omega$)	4 × 1	30	−70.00	−50.00	+50.00
Present ($10\beta - 5\omega$)	8 × 2	81	−74.48	−50.00	+50.00
Present ($10\beta - 5\omega$)	16 × 4	255	−80.34	−50.00	+50.00
Yunus (Mixed AQ)	4 × 1, dist.	30	−70.30	−50.60	+50.80
Yunus et al. (AQ)	4 × 1, dist.	30	−70.50	−53.60	+46.00
Present ($8\beta - 3\omega$)	4 × 1, dist.	20	−65.01	−45.83	+45.83
Present ($10\beta - 5\omega$)	4 × 1, dist.	30	−64.27	−41.87	+41.23

or even good (Yunus 1988; Yunus et al. 1989) results; therefore it seems reasonable to state that the locking effect is more likely due to the displacement model than to the stress model chosen.

5.5 *A thick cantilever beam*

In this case a shear-loaded cantilever beam is analyzed, and the results, in terms of average tip displacement, are checked against the theoretical value obtained for a Timoshenko beam. Geometry and load condition are reported in Fig. 5; the material properties are $E = 30000$, $\nu = 0.25$. Some regular and one distorted mesh are considered and the relative response of the numerical simulations can be found in Figs. 6 and 7. The present elements perform well and, even in the distorted case (the relative error is less than 7% for the 8 DOFs models—a better result, if compared with other similar available elements, and obtained with a lower number of DOFs—and about 10% for the 12 DOFs one). Comparison in terms of stress computations is presented in Table 6.

5.6 *Cook's problem*

This tapered panel with one edge fixed and the opposite subjected to a uniform shear load (see Fig. 8) was first proposed as a test problem by Cook (1974) and is considered a useful tool to evaluate the performance of membrane elements in presence of a distorted mesh under combined bending and shear stresses. No analytical solution is available for this problem, so the results in Fig. 9 and in Table 7 (stresses) are compared with a "best value" obtained through a refined numerical analysis. The material properties are $E = 1$, $\nu = 1/3$. The response of the proposed elements, especially of those with 8 DOFs, is fairly accurate, comparable with that produced by the models M1 and M2 of the paper by Iura and Atluri (1992) which, on the other side, have 12 DOFs; in Fig. 9 the convergence plots show that a substantial saving can be achieved if the new 8 DOFs element are adopted.

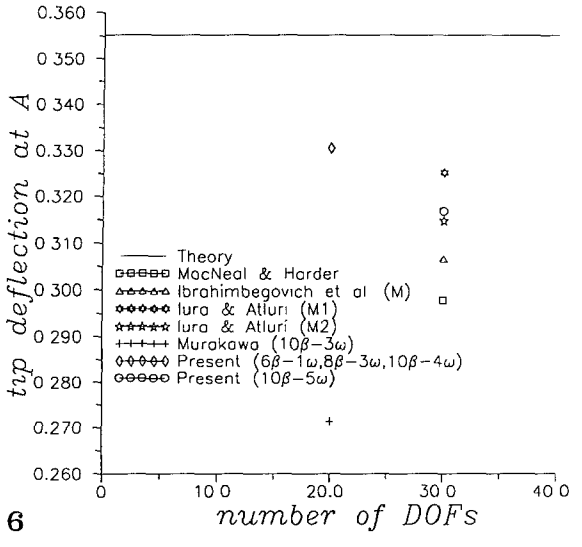

6

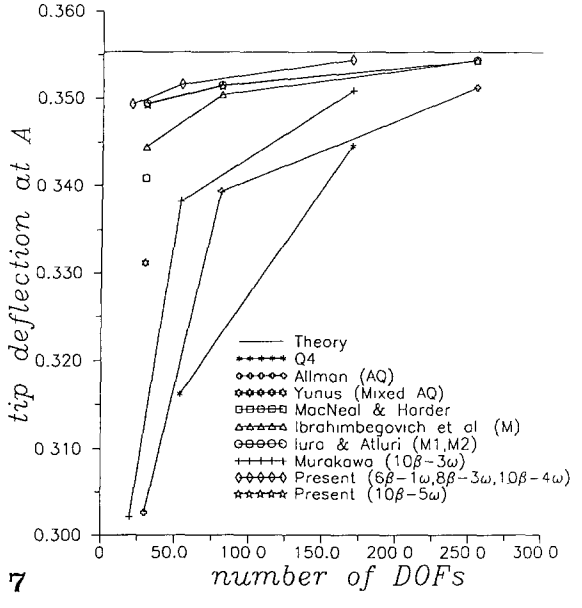

7

Figs. 6 and 7. Convergence plots (**6** with regular mesh and **7** with distorted mesh) for the shear-loaded thick cantilever beam problem

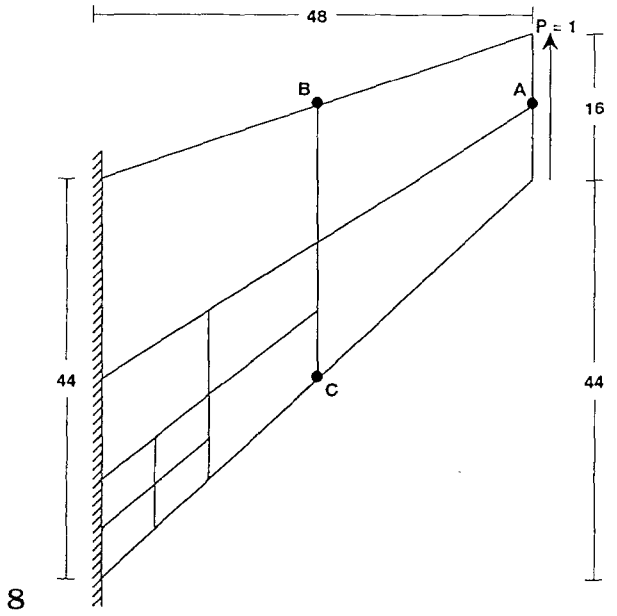

8

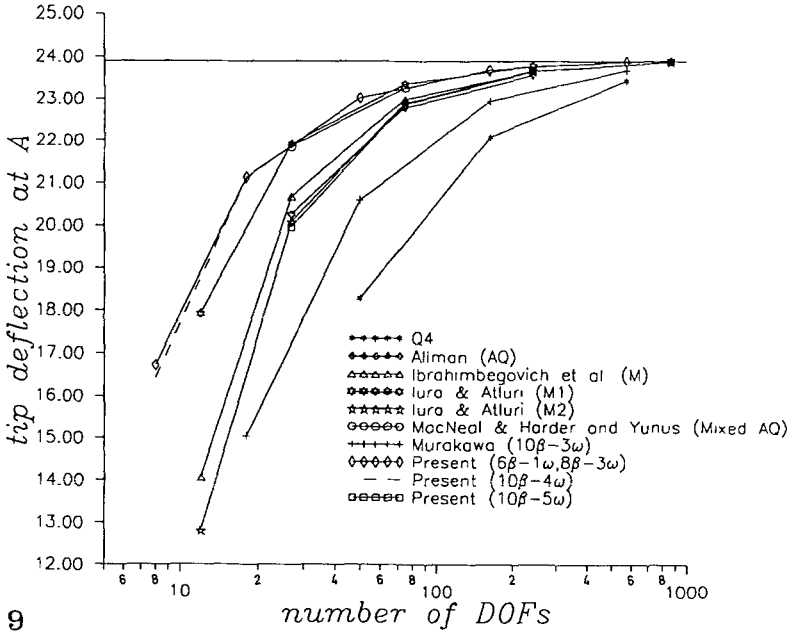

9

Figs. 8 and 9. **8** Geometry and loads for the analysis of the Cook's problem. Tip deflection is evaluated at point *A*, while point *B*, *C* are used for stress computations. The pattern of mesh refinement is partially shown. **9** Convergence plots for the Cook's problem

6 Conclusions

A Hellinger–Reissner type variational principle is presented which allows to develop membrane elements where a priori unsymmetric stress components and drilling DOFs, as well as the traditional displacement DOFs, are the independent variables. The AMB condition is one of the Euler–Lagrange equations of the functional, so the symmetry of the stress tensor, at least in a weak sense, is guaranteed a posteriori, once stationarity is enforced. Provided that no zero energy modes are introduced, there are no restrictions on the choice of the shape functions which define the stress, rotation and displacement fields.

In order to achieve a reasonably good level of accuracy with a small number of nodal parameters, a family of 4-noded elements has been developed, with several selections of rotation and

Table 7. Values of minimum principal stress at B and maximum principal stress at C for the Cook's problem; the best known solution was obtained by Bergan and Felippa with a refined 32 × 32 mesh

Element	Mesh	No. of DOFs	$\sigma_{min,B}$	$\sigma_{max,C}$
Best known solution	—	—	−0.2012	+0.2359
Allman (AQ)	2 × 2	27	−0.1716	+0.1825
Allman (AQ)	4 × 4	75	−0.1921	+0.2261
Allman (AQ)	8 × 8	243	−0.2004	+0.2340
Yunus (Mixed AQ)	2 × 2	27	−0.1763	+0.1849
Yunus (Mixed AQ)	4 × 4	75	−0.1944	+0.2225
Present ($8\beta - 3\omega$)	1 × 1	8	−0.1204	+0.1937
Present ($8\beta - 3\omega$)	2 × 2	18	−0.1549	+0.1854
Present ($8\beta - 3\omega$)	4 × 4	50	−0.1856	+0.2241
Present ($8\beta - 3\omega$)	8 × 8	162	−0.1986	+0.2344
Present ($8\beta - 3\omega$)	16 × 16	578	−0.2025	+0.2364
Present ($10\beta - 5\omega$)	2 × 2	27	−0.1591	+0.1746
Present ($10\beta - 5\omega$)	4 × 4	75	−0.1864	+0.2251
Present ($10\beta - 5\omega$)	8 × 8	243	−0.1985	+0.2346
Present ($10\beta - 5\omega$)	16 × 16	867	−0.2024	+0.2365

(least-order) stress models; stress components are defined in natural convected coordinates, but referred to a centroidal base system, in order to pass the patch test. In some cases it is possible to express the rotation parameters in terms of nodal rotations, and also to add these drilling DOFs to the DOFs coming from the displacement field, so that an element with 3 DOFs per node can be formulated. Even if the performance of such an element are often not as good as that of elements where rotation parameters are condensed, nevertheless it may be useful as the basis of a flat faceted element for analysis of curved membranes, where the presence of additional connectors in the form of drilling rotations could improve the smoothness of the solution. On the other hand, when the rotation parameters are condensed, the presence of higher order stress modes is not going to stiffen the element, as it might be otherwise expected.

The elements have been compared with other membrane models based on mixed or hybrid variational principles to point out differences and similarities, with particular reference to elements with drilling DOFs and to the standard 4-noded displacement-based isoparametric formulation (Q4).

Some benchmark problem have been solved to check the reliability of the new elements; results of the numerical study show that the performance is, in almost all cases considered, excellent.

Acknowledgements

This work was supported by NASA Langley Research Center, with Dr. Jerold Housner as the program official, and by the Italian National Research Council (C.N.R.). This support is gratefully acknowledged.

References

Allman, D. J. (1984): A compatible triangular element including vertex rotations for plane elasticity analysis. Comp. and Struct. 19, 1–8

Allman, D. J. (1988): A quadrilateral finite element including vertex rotations for plane elasticity analysis. Intern. J. Numer. Meth. Eng. 26, 717–730

Atluri, S. N. (1979): On rate principles for finite strain analysis of elastic and inelastic nonlinear solids. In: recent research on mechanical behaviour. pp 79–107, University of Tokyo Press, Tokyo

Atluri, S. N. (1980): On some new general and complementary energy theorems for the rate problems in finite strain, classical elastoplasticity. J. Struct. Mech. 8, 61–92

Atluri, S. N. (1984): Alternate stress and conjugate strain measures, and mixed variational formulations involving rigid rotations, for computational analyses of finitely deformed solids, with application to plates and shells—I Theory. Comp. and Struct. 18, 98–116
Atluri, S. N.; Murakawa, H. (1977): On hybrid finite element models in nonlinear solid mechanics. In: Bergan, P. G. et al. (eds): Finite elements in nonlinear mechanics. Tapir Press, Norway 1, 25–69
Bergan, P. G.; Felippa, C. A. (1985): A triangular membrane element with rotational degrees of freedom. Comp. Meth. Appl. Mech. Eng. 50, 25–69
Cook, R. D. (1974): Improved two dimensional finite elements. ASCE J. Struct. Div. ST6, pp 1851–1863
Cook, R. D. (1981): Concepts and applications of finite element analysis. (2nd ed). Wiley: New York
Cook, R. D. (1986): On the Allman triangle and a related quadrilateral element. Comp. and Struct. 22, 1065–1067
Cook, R. D. (1987): A plane hybrid element with rotational d.o.f. and adjustable stiffness. Intern. J. Numer. Meth. Eng. 24, 1499–1508
Fraeijs de Veubeke, B. M. (1975): Stress function approach. Proceedings of world congress of finite element methods in Structural Mechanics, Bournemouth, U.K., pp J1–J51
Fraeijs de Veubeke, B. M.; Millard, A. (1976): Discretization of the stress fields in the finite element method. em Journal of the Franklin Institute. 302, 389–412
Ibrahimbegovich, A.; Taylor, R. L.; Wilson, E. L. (1990): A robust quadrilateral membrane finite element with drilling degrees of freedom. Intern. J. Numer. Meth. Eng. 30, 445–457
Iura, M.; Atluri, S. N. (1992): Formulation of a membrane finite element with drilling degrees of freedom. Comp. Mech. 9, 417–428
MacNeal, R. H.; Harder, R. L. (1985): A proposed standard set of problems to test finite element accuracy. Finite elements in analysis and design. 1, 3–20
MacNeal, R. H.; Harder, R. L. (1988): A refined four-noded membrane element with rotational degrees of freedom. Comp. and Struct. 28, 75–84
Murakawa, H. (1978): Incremental hybrid finite element methods for finite deformation problems (with special emphasis on complementary energy principle). Ph.D. Thesis, Georgia Institute of Technology
Murakawa, H.; Atluri, S. N. (1978): Finite elasticity solutions using hybrid finite elements based on a complementary energy principle. ASME J. Appl. Mech. 45, 539–547
Murakawa, H.; Atluri, S. N. (1979): Finite elasticity solutions using hybrid finite elements based on a complementary energy principle. Part 2: incompressible materials. ASME J. Appl. Mech. 46, 71–77
Pian, T. H. H. (1964): Derivation of element stiffness matrices by assumed stress distributions. AIAA J. 2, 1333–1336
Pian, T. H. H. (1985): Finite elements based on consistently assumed stresses and displacements. Finite Elements in Analysis and Design 1, 131–140
Pian, T. H. H.; Chen, D. (1983): On the suppression of zero energy deformation modes. Intern. J. Numer. Meth. Eng. 19, 1741–1752
Pian, T. H. H.; Sumihara, K. (1984): Rational approach for assumed stress finite elements. Intern. J. Numer. Meth. Eng. 20, 1685–1695
Pian, T. H. H.; Tong, P. (1986): Relations between incompatible displacement model and hybrid stress model. Intern. J. Numer. Meth. Eng. 22, 173–181
Pian, T. H. H.; Wu, C.-C. (1988): A rational approach for choosing stress terms for hybrid finite element formulations. Intern. J. Numer. Meth. Eng. 26, 2331–2343
Punch, E. F. (1983): Stable, invariant, least-order isoparametric mixed-hubrid stress elements: Linear elastic continua, and finitely deformed plates and shells. Ph.D. Thesis, Georgia Institute of Technology
Punch, E. F.; Atluri, S. N. (1984): Development and testing of stable, invariant, isoparametric curvilinear 2- and 3-D hybrid stress elements. Comp. Meth. Appl. Mech. Eng. 47, 331–356
Reissner, E. (1965): A note on variational principles in elasticity. Intern. J. Solids Struct. 1, 93–95
Rubinstein, R.; Punch, E. F.; Atluri, S. N. (1983): An analysis of, and remedies for, kinematic modes in hybrid-stress finite elements: selection of stable, invariant stress fields. Comp. Meth. Appl. Mech. Eng. 38, 63–92
Wu, C.-C.; Huang, M.-G.; Pian, T. H. H. (1987): Consistency condition and convergence criteria of incompatible elements: general formulation of incompatible functions and its application. Comp. and Struct. 27, 639–644
Yunus, S. M. (1988): A study of different hybrid elements with and without rotational d.o.f. for plane stress/plane strain problems. Comp. and Struct. 30, 1127–1133
Yunus, S. M.; Saigal, S.; Cook, R. D. (1989): On improved hybrid finite elements with rotational degrees of freedom. Intern. J. Numer. Meth. Eng. 28, 785–800

Communicated by S. N. Atluri, August 13, 1992